Kovove Mater. 62 2024 377–387
DOI: 10.31577/km.2024.6.377

Effects of ultrasonic peening on corrosion fatigue and corrosion behavior of welded AA5086-H32 aluminum alloy

Recep Sadeler[1]*, Hakan Erge[1], Selçuk Atasoy[2]

[1] *Department of Mechanical Engineering, Ataturk University, Erzurum, Turkey*
[2] *Department of Mechanical Engineering, Giresun University, Giresun, Turkey*

Received 14 October 2024, received in revised form 12 November 2024, accepted 14 November 2024

Abstract

Ultrasonic peening (UP) is a method that has been increasingly used in recent years to improve the fatigue strength of welded joints and structures. This study investigated the fatigue strength of butt-welded AA5086-H32 aluminum alloy plate specimens and the effects of ultrasonic peening under atmospheric and corrosive conditions. Exfoliation, intergranular, and electrochemical corrosion tests were also conducted further to analyze the effects of ultrasonic peening on corrosion behavior. Results demonstrated that the peening treatment enhanced the fatigue strength in air and corrosion conditions. The improvement can be attributed to surface layer hardening and applying compressive residual stresses to reduce stress concentration. Peening treatment also reduces corrosion sensitivity through surface hardening.

K e y w o r d s: ultrasonic peening (UP), corrosion fatigue strength, AA5086-H32 aluminum alloy, butt weldment, intergranular corrosion, electrochemical corrosion

1. Introduction

Aluminum alloys, especially the 5xxx series, are increasingly being utilized in the transportation manufacturing industries, including shipbuilding, railway vehicles, automotive, and aerospace, due to their lightweight properties, high specific strength, and corrosion resistance [1]. The components of these transport machines are often constructed using fusion welding technologies. Transportation machinery structures often experience cyclic loading, resulting in fatigue failure. Therefore, fatigue behavior in aluminum alloy weldments is a critical issue that needs to be addressed in structural design.

The fatigue strength of aluminum alloy welded joints is lower than that of non-welded plates. Three factors mainly induce this reduced fatigue strength: (1) tensile residual stress along the weld line, (2) stress concentration at the weld tip, and (3) softening of the weld metal (WM) zone and heat-affected zone (HAZ) [2–5]. Thus, fatigue fractures of welded parts usually occur at the weld tip, where there is high local stress and low stiffness [6, 7]. Various surface treatment technologies, such as ball polishing, shot peening, or other methods that induce plastic deformation in the surface layer, have been applied to improve the reduced fatigue strength of the weld. Several studies have reported that the fatigue strength of the weld can be improved through these surface treatments, mainly due to the induction of compressive residual stress and work hardening [7–9]. One application that achieves this is the ultrasonic peening (UP) process, which introduces compressive residual stresses on the material surface, thereby counteracting tensile residual stresses. The beneficial effect of UP lies in its ability to reduce stress concentration at the weld toe in welded materials and to improve the mechanical properties of the material surface. Studies on the fatigue behavior of welded specimens have shown that, compared to conventional methods such as heat treatment, hammer peening, shot peening, and grinding, UP is the most effective method [10].

Handling machines are often exposed to corrosive environments during service, such as ships that are frequently in contact with seawater. Therefore, improving the corrosion fatigue behavior of aluminum alloy welds by surface treatments is an important issue to clarify for structural design. Corrosion fatigue

*Corresponding author: tel.: +90 442 231 4841; e-mail address: receps@atauni.edu.tr

Table 1. Chemical composition of the 5086 aluminum alloy plate and the welding wire ER5336 used (wt.%)

Alloy	Si	Fe	Cu	Mn	Mg	Zn	Cr	Ti	Zr	Al
AA5086	0.17	0.45	0.028	0.58	4.46	0.13	0.073	0.019	–	Remaining
ER5356	0.041	0.11	< 0.005	0.15	4.82	< 0.005	0.13	0.10	–	Remaining

Table 2. Mechanical properties of the material used

Yield strength	Tensile strength	Elongation	Young's modulus
150 MPa	280 MPa	20 %	71 GPa

Table 3. Welding conditions

Voltage	Current	Wire feed speed	Welding speed
19.5 V	125–135 A	9.5 m min^{-1}	36.5 cm min^{-1}

has been observed to significantly deteriorate the fatigue strength of both welded and non-welded plates in a simulated seawater environment (3.5 % NaCl solution) compared to those tested in air [11, 12]. The formation of corrosion pits associated with precipitates in the aluminum matrix under corrosive environments can reduce the crack initiation life and subsequently reduce the fatigue life and strength of the material [11, 13].

The UP process is applied using a rod or pin that oscillates at low amplitude and high frequency, inducing ultrasonic vibrations on the material surface. This causes significant plastic deformation in the surface layers, leading to grain refinement, microstructural improvement, and geometric modification. Additionally, the plastic deformation helps close microcracks on the material surface that would otherwise reduce corrosion resistance, fatigue life, and strength. Harmful tensile residual stresses in the surface layers are also relieved and replaced with beneficial compressive residual stresses. As a result, the UP process increases surface microhardness and enhances the material's strength and corrosion fatigue resistance [14].

In addition, welded joints often exhibit lower corrosion resistance than the base material due to high residual stresses generated during cooling and solidification. Therefore, recent studies have focused on enhancing fatigue strength through various post-weld surface treatments. Processes like UP, in particular, can refine grains in the material after welding and improve the corrosion resistance of the structures [15].

As discussed above, many studies have been conducted on the effects of surface treatments on both the fatigue strength of aluminum alloy welds in air and the corrosion fatigue behavior of untreated aluminum alloy welds. However, to date, only a few studies have investigated the combined effect of surface treatment on the corrosion fatigue behavior of aluminum alloy welded parts. Furthermore, the respective roles of surface hardening and compressive residual stress induced by surface treatment have not been fully elucidated, even though these factors are known to be the primary reasons for improving fatigue strength through surface treatment.

In the present study, fatigue tests were conducted on butt-welded AA5086-H32 aluminum alloy plate specimens with and without ultrasonic peening in both air and 3.5 % NaCl solution. This study aimed to investigate the effects of surface treatment on the corrosion fatigue behavior of aluminum alloy weldments. The respective roles of surface hardening and compressive residual stress induced by the peening treatment have also been discussed in detail in this study. Additional corrosion tests were conducted to investigate the effect of peening treatment on corrosion behavior and the effect of corrosion behavior on corrosion fatigue behavior.

2. Experimental procedures

2.1. Material and specimen

In this study, AA5086-H32 aluminum alloy plates with a thickness of 5 mm, length of 50 mm, and width of 15 mm were used as the base metal. The chemical composition and mechanical properties of the material used are shown in Tables 1, 2.

A groove with an angle of 90° was machined on the edge perpendicular to the rolling direction of the plate. The two plates were then butt-welded using an ESAB MIG 5000i model welding machine. The butt-welding process and sample dimensions are shown schematically in Fig. 1. The welding conditions are presented

Table 4. Ultrasonic peening (UP) process parameters

Air pressure	Frequency	Amplitude	Time	Pulse Needle shape	Impact location
4 bar	19 ± 1 kHz	40 µm	5 min	Circular D (Diameter) 1.5 mm	Single surface

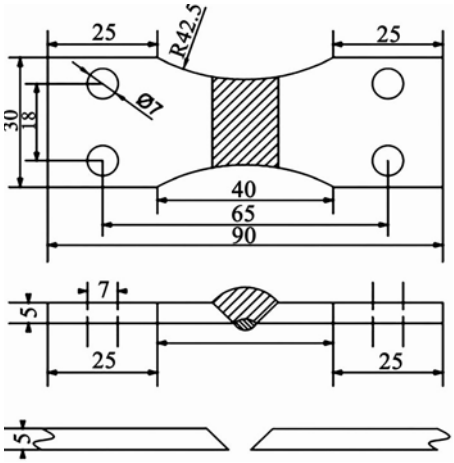

Fig. 1. Schematic overview of the welded plate and sample dimensions.

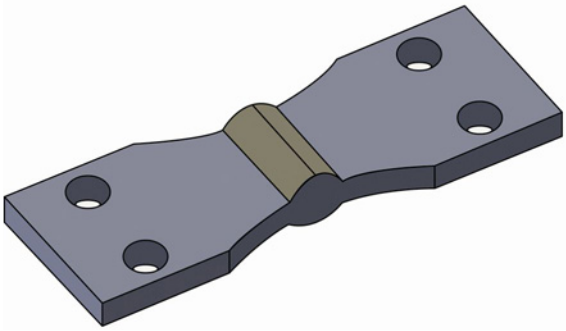

Fig. 2. Schematic view of the fatigue test specimen for plane bending cyclic loading.

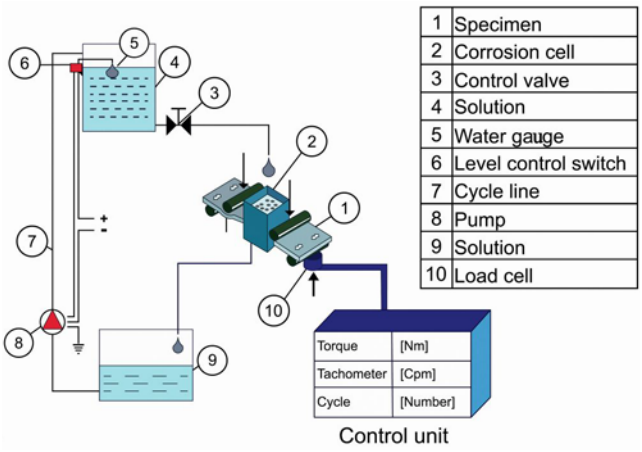

Fig. 3. Schematic view of the corrosion fatigue test set-up.

in Table 3, and the chemical composition of the welding wire (ER5356) with a diameter of 1.6 mm is shown in Table 1.

The microstructure of the welded specimen without peening was observed using a scanning electron microscope (SEM) to identify the regions of weld metal (WM), heat-affected zone (HAZ), and base metal (BM). The hardness distributions in the welding region for both welded specimens with and without peening were measured using a hardness tester with a load of 200 gf and a hold time of 10 s. The hardness measurement was made on the specimen surface to determine the effect of the peening surface treatment.

2.2. Fatigue tests

Fatigue specimens for plane bending fatigue tests were cut from the welded plates. The specimens had a width of 30 mm at the minimum section in the center region, a length of 90 mm, and a thickness of 5 mm. The schematic geometry of the specimens is shown in Fig. 2.

The ultrasonic peening treatment was applied to the welded specimens using a Sonata Nomad HFMI type Ultrasonic Peening equipment to investigate its effect on corrosion fatigue behavior. The ultrasonic peening (UP) parameters are provided in Table 4. UP parameters were determined based on knowledge of literature and industry practices.

Four types of fatigue tests were conducted: (1) welded specimens tested in air, (2) welded specimens tested under 3.5 % NaCl solution, (3) welded and ultrasonic-peening specimens tested in air, and (4) welded and ultrasonic-peening specimens tested under 3.5 % NaCl solution. Fatigue tests were carried out using a plane bending fatigue machine at a stress ratio of $R = 0$ and a frequency of 19 Hz. The specimens were immersed in 3.5 % NaCl solution for corrosion fatigue tests, as shown in Fig. 3.

The fatigue tests were conducted at stress ranges ($\Delta\sigma$) ranging from 110 to 160 MPa in air and corrosive environments, with three repetitions at each specified stress level during the experiments. After the fatigue test, the surfaces of the specimens near the fracture location and the fracture surfaces were carefully examined using a scanning electron microscope (SEM) to investigate the fatigue crack initiation location and

mechanism, as well as the influence of corrosion behavior on them.

2.3. Corrosion tests

Samples with a length of 50 mm, a width of 15 mm, and a thickness of 5 mm were cut from the welded plate for corrosion tests. The corrosion tests were conducted under a 3.5 % NaCl solution prepared by ASTM G66 [16] and ASTM G67 [17] standards.

The exfoliation corrosion susceptibility of the samples was evaluated by immersing them in the corrosive solutions according to the ASTM-G66 standard [16].

The nitric acid mass loss test (NAMLT), according to the ASTM-G67 standard, was performed to investigate the intergranular corrosion behavior of AA5xxx aluminum alloys. This test method involves measuring the weight loss of the sample before and after the test [17].

Electrochemical corrosion tests were conducted in a 3.5 % NaCl solution using an electrochemical corrosion cell with three electrodes: a working electrode, a reference electrode, and a counter electrode. The potential difference between the working electrode (the sample) and the reference electrode was varied to measure the current and potential between the counter and working electrodes. A platinum counter electrode was used in the test.

3. Results and discussion

3.1. Microstructure and hardness distribution of the welded specimen

In Figs. 4a–c, the WM, HAZ, and BM microstructures for the welded sample are shown. It can be observed that the WM region had a coarse solidified microstructure, whereas the HAZ region showed two different microstructure regions, one with coarser grains and the other with finer grains, depending on the difference in heating temperature from the welding center.

Figure 5 presents the hardness distributions of the welded specimens with and without peening treatment. The figure indicates that the hardness in the WM region was the lowest due to the coarse solidified microstructure. The hardness in the HAZ region displayed a two-step distribution, which corresponds to the two regions of grain size observed in Figs. 5a–c: the lower hardness region corresponds to the coarser grain size region, and the higher hardness region corresponds to the finer grain size region. The hardness in the BM region was the highest due to no influence of heating during welding. The shape of the hardness distribution was similar between the two welded specimens with and without peening treatment, while the peening treatment increased the hardness by approximately 10 to 13 HV.

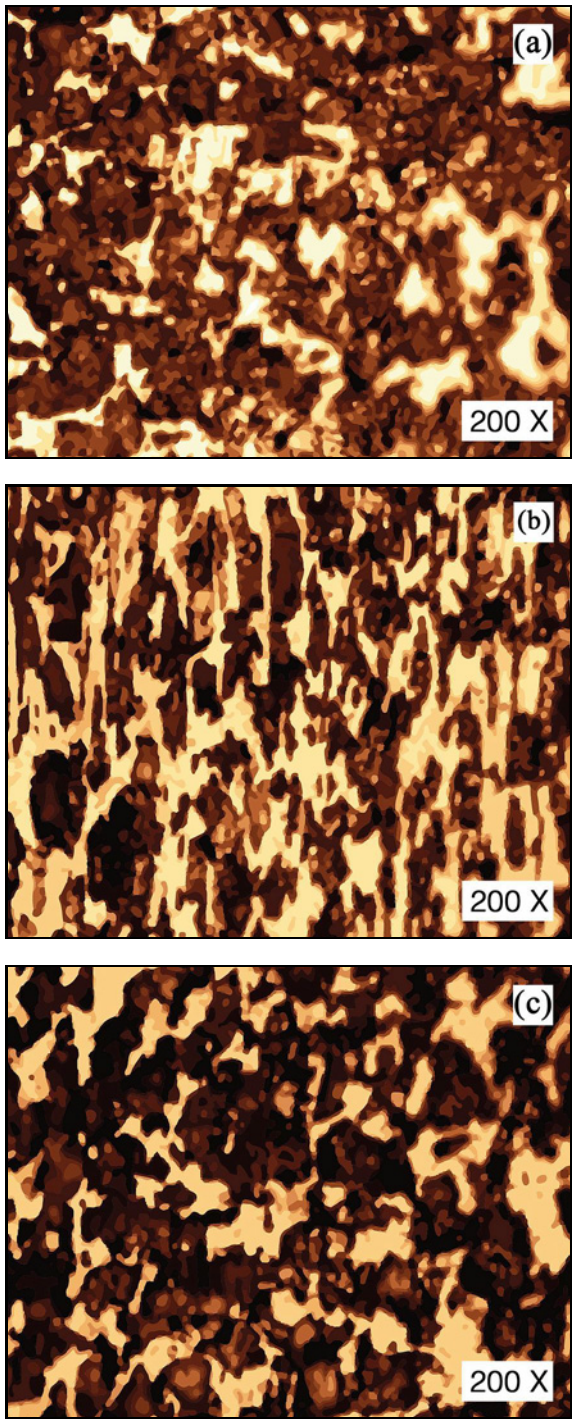

Fig. 4. Microstructures of (a) BM, (b) HAZ, and (c) WM for the welded sample.

The shapes of the hardness distributions reported in this study are similar to those reported in previous studies [18–20]. Additionally, the hardness level of TIG welding is higher than that of MIG welding [20], which may be attributed to the difference in heat in-

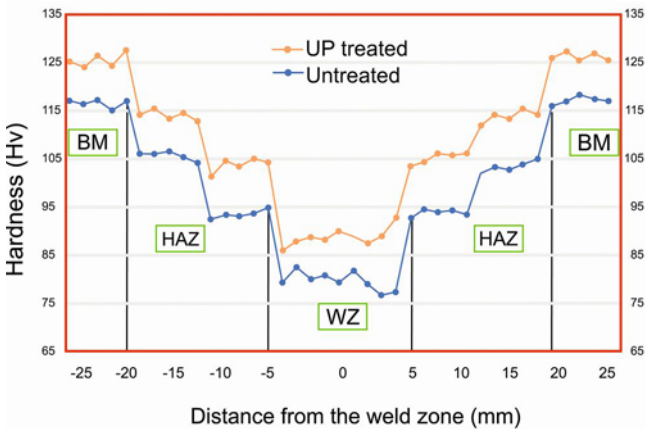

Fig. 5. Hardness distribution of the welded 5086-H32 aluminum alloys with and without peening treatment.

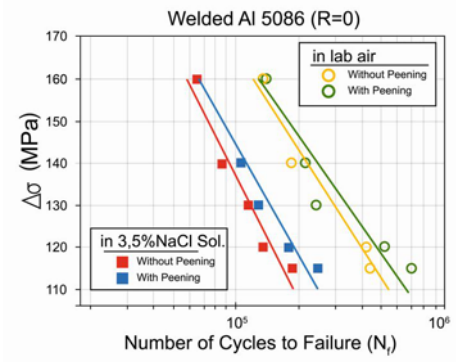

Fig. 6. *S-N* curves for the welded specimens with and without peening treatment tested in air and 3.5 % NaCl solution.

put between the two methods. Moreover, the hardness of the welded and peening specimens is higher than that of the welded specimens without peening treatment. The higher hardness results from the hardening of the surface layer and the compressive residual stress induced by peening [21].

3.2. Fatigue and corrosion fatigue behavior

The results of the four types of fatigue tests are presented in Fig. 6. As shown, the fatigue strength of the welded specimen with peening treatment in the air is relatively high but almost the same as that of the welded specimen without peening treatment. Although peening treatment is known to increase surface hardness and induce compressive residual stress on the surface, these effects on hardness and residual stress are likely too small to significantly influence the fatigue strength within the range of the present study.

Regarding residual stress, there are two types of residual stress present in the specimen: tensile residual stress due to butt-welding and compressive residual stress due to peening treatment. It is speculated that the tensile residual stress resulting from butt-welding will be relieved when removing the small specimen from the large plate, and as a result, the residual stress will become small enough [22, 23]. On the other hand, as shown in Fig. 6, the fatigue strengths of the welded specimen with peening treatment at lower stress ranges are significantly higher than those of the welded specimen without peening treatment. However, at higher stress ranges, the fatigue strengths become similar, which is a common trend in the residual stress effect on fatigue strength. This suggests that the compressive residual stress induced by the peening treatment plays a role. Regarding the effect of increased surface hardness due to the peening treatment on fatigue strength in air, as shown in Fig. 5, it is speculated to be negligible based on the fatigue test results shown in Fig. 6. Furthermore, as shown in Fig. 6, the fatigue strengths of the welded specimens in 3.5 % NaCl solution are lower than those in air, regardless of whether peening treatment is applied or not. Notably, this result suggests that the decrease in fatigue strength in the 3.5 % NaCl solution is more significant for the welded specimen without peening treatment than for the welded specimen with peening treatment, indicating that peening treatment can enhance corrosion fatigue strength. This finding is consistent with numerous previous studies [24–26], which have reported that peening treatments can improve corrosion fatigue strength by inducing increased hardness and compressive residual stress. However, the specific mechanisms through which these effects operate, such as the dominant effect or how these effects interact, remain unclear. As previously discussed, the impact of the incremental changes in residual stress and hardness is expected to be minor or insignificant in the current study conducted in the air. Since the effect of residual stress as a mechanical factor would be consistent in both environments and relatively small, the greater fatigue strength in 3.5 % NaCl solution for the welded specimen with peening treatment compared to that without peening treatment can be attributed to the increased surface hardness with finer grains resulting from the peening treatment.

The fracture location for all four cases was at the weld toe, the fusion boundary between the weld metal and HAZ. The weld toe is a well-known position of high-stress concentration that initiates fatigue crack. Therefore, in air, the fracture locations for the welded specimens with and without peening treatment were at the weld toe, which is the highest stress location. Since the highest stress and corrosion occurred at the weld toe, fracture locations in the welded specimens tested in 3.5 % NaCl solution were also at the weld toe.

Figures 7a–d illustrate the surface morphology of

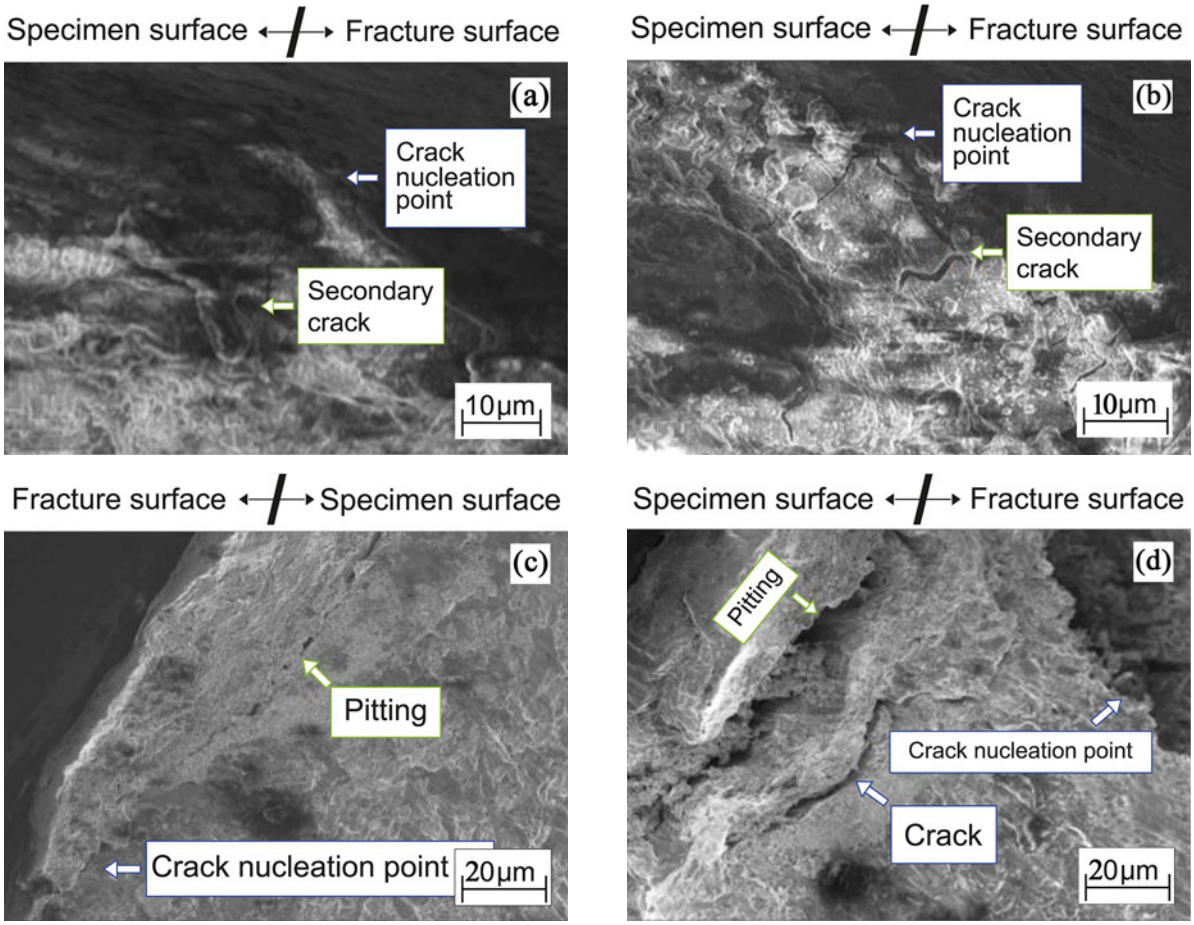

Fig. 7. Observations of corroded specimen surface near the fracture location: (a) without peening treatment in air, (b) with peening treatment in air, (c) without peening treatment in air, and (d) with peening treatment in 3.5 % NaCl solution.

Table 5. Chemical materials used in the exfoliation corrosion test

	Molecular weight	Molarite	Quantity
$NH_{42}Cl$ (ammonium chloride)	53.49 g mol^{-1}	1.0 M	53.5 g
NH_4NO_3 (ammonium nitrate)	80.04 g mol^{-1}	0.25 M	20.0 g
$(NH_4)_2C_4H_4O_6$ (ammonium tartrate)	184.15 g mol^{-1}	0.01 M	1.8 g
30% H_2O_2 (hydrogen peroxide)	34.01 g mol^{-1}	0.09 M	10 ml

the specimens near the fracture point after fatigue tests in air and 3.5 % NaCl solution, respectively. The observed locations were in the weld-toe region, corresponding to the fusion line zone mentioned previously. As shown, corrosion pits and cracks from defect coalescence were observed in the 3.5 % NaCl solution but were absent in the fatigue tests conducted in the air. It is unclear from Figs. 7c,d whether the peening treatment can improve corrosion behavior. This is because the corrosion fatigue crack typically initiates from pits or corrosion defects that form during the fatigue cycles, resulting in a similar surface morphology for both peened and unpeened specimens after the tests. To clarify the effect of peening treatment on corrosion behavior, three types of corrosion tests were conducted on the welded specimens with and without peening treatment, which will be discussed in the next section.

3.3. Corrosion test results

3.3.1. Exfoliation corrosion (EXCO) test

The exfoliation corrosion susceptibility of AA5086 aluminum alloy was evaluated using an immersion test according to ASTM G66. Before the test, the cut samples were cleaned by wet polishing with 400, 800, 1000, and 1200 grit sandpapers. The chemicals used for the corrosion tests are listed in Table 5. Based on the detailed observations of the samples after the exfoliation

Table 6. NAMLT test results for the welded samples with and without peening treatment

	Surface area	Weight before test	Weight after test	Weight difference	Weight loss
Without peening	19.86 cm^2	7.3341 g	6.5648 g	769.3 mg	38.73 mg cm^{-2}
With peening	19.86 cm^2	7.4795 g	6.8048 g	674.7 mg	33.97 mg cm^{-2}

corrosion tests, no exfoliation behavior, which refers to lamellar cracking parallel to the sample surface, was observed for both the samples with and without peening treatment under all four types of solutions. This result is consistent with other studies reported in the literature [27, 28].

3.3.2. Intergranular corrosion test

A Nitric Acid Metal Loss Test (NAMLT) was conducted according to ASTM G67 standard by immersing the samples in 70 % concentrated nitric acid. Before the test, the sample surface was cleaned by wet polishing with 400, 800, 1000, and 1200 grit sandpapers. The surface area of the sample was measured with an accuracy of 19.86 cm^2, and the weight was determined using a precision balance before immersion. After the test, the weight was measured again to evaluate the weight loss. The results of the test for the welded samples with and without peening treatment are shown in Table 6. The results indicate that the weight loss for the peening sample was lower than that of the unpeened sample. Therefore, it can be concluded that the ultrasonic peening treatment enhances the intergranular corrosion resistance of the welded AA5086 aluminum alloy.

The sample surfaces were examined after the test to observe the details of the intergranular corrosion behavior, as shown in Figs. 8a–c and Figs. 9a–c for the unpeened and peened samples, respectively. As observed from the figures, the intergranular corrosion was most significant in the weld metal, followed by the heat-affected zone, and least in the base metal, irrespective of the peening treatment. Since the corrosion fatigue crack initiated at the fusion line between the heat-affected zone and weld metal in the current experiment, the corrosion defects formed due to the intergranular corrosion may be one of the potential factors that degrade the fatigue strength of the unpeened sample compared to the peened sample.

According to Goyal and Garg [29], the weight loss obtained by the same NAMLT test for the friction weldment of AA5086 aluminum alloy was between 6 and 8 mg cm^{-2}. Hans and Banjwa [30] found a mass loss of 33.36 mg cm^{-2} for TIG welded AA5086 aluminum alloy and 11.07 mg cm^{-2} for friction stir welding of the same material. Based on these results and the present study, fusion weldments with high heat input, such as MIG and TIG welding, may have lower intergranular corrosion resistance than solid weldments

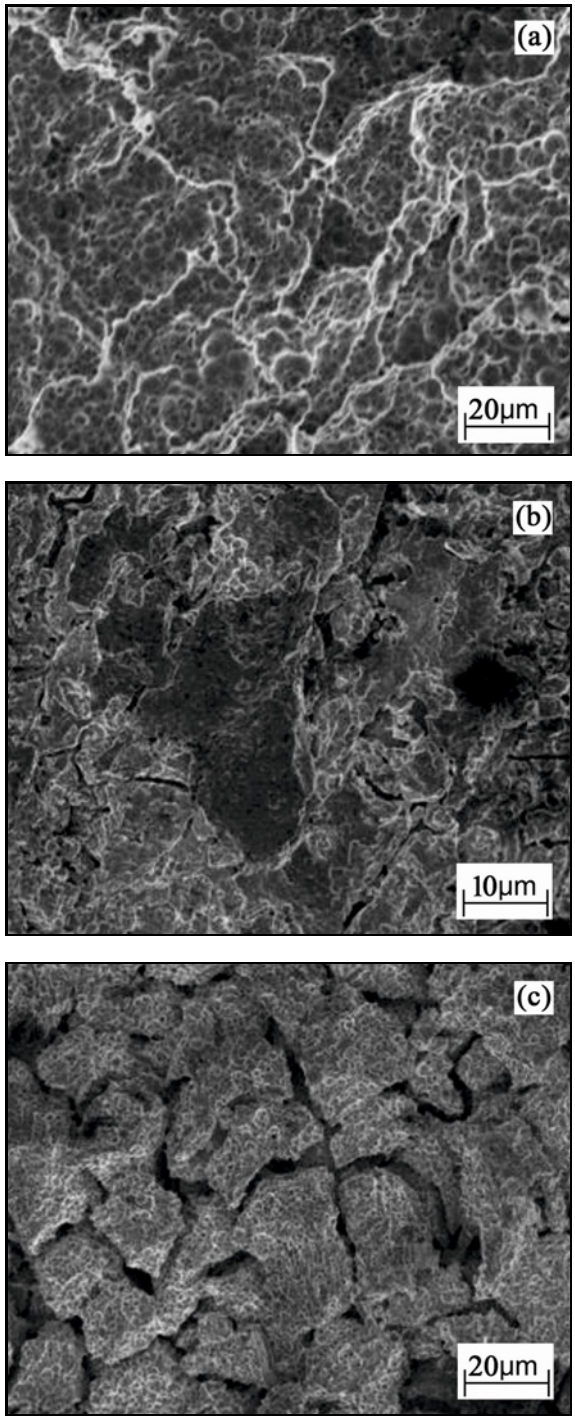

Fig. 8. Surface observations of the sample without peening treatment after the intergranular corrosion test according to ASTM G67: (a) BM region, (b) HAZ region, and (c) WM region.

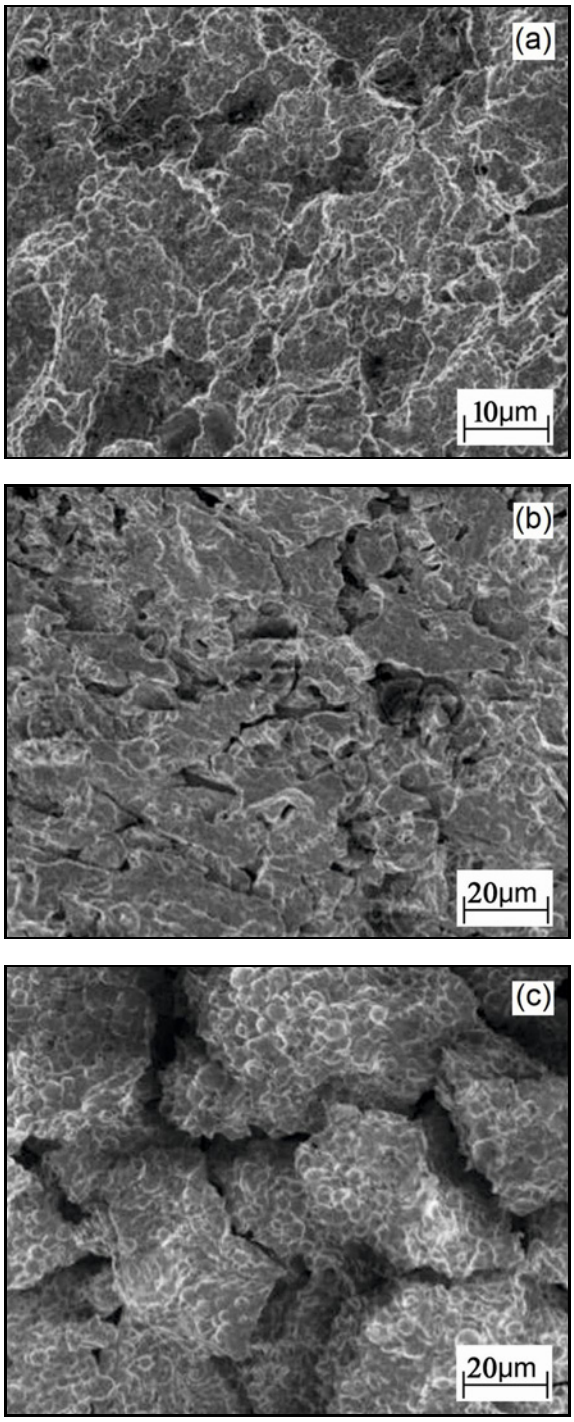

Fig. 9. Surface observations of the sample with peening treatment after the intergranular corrosion test according to ASTM G67: (a) BM region, (b) HAZ region, and (c) WM region.

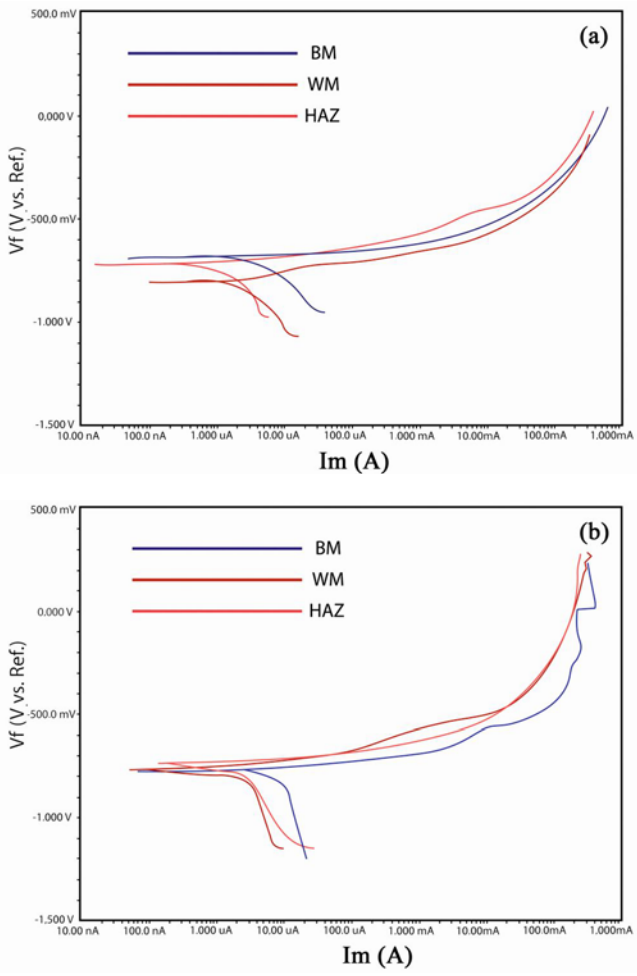

Fig. 10. Potentiostat curves for the welded samples: (a) without peening treatment and (b) with peening treatment.

or those with less fusion, such as friction welding or friction stir welding. Microstructure coarsening caused by high heat input in fusion welding may also influence intergranular corrosion behavior, and high temperatures during fusion welding have been reported to increase the sensitivity of intergranular corrosion [31]. Regarding the effect of peening on intergranular corrosion behavior, the plastic deformation of the surface layer induced by peening may lead to changes in microstructure and high hardness, contributing to higher intergranular corrosion resistance. Additionally, the compressive residual stress induced by peening may contribute to improved intergranular corrosion resistance to some extent.

3.3.3. Electrochemical corrosion test

The electrochemical corrosion test results show the potentiostat curves for the welded samples without peening in Fig. 10a. The blue, orange, and red curves represent the base metal (BM), heat-affected zone (HAZ), and weld metal (WM), respectively. The figure indicates that the corrosion resistance of the WM is the lowest, while that of the HAZ is intermediate, and that of the BM is the highest. The low corro-

Table 7. The improvement rate of fatigue life ΔN_f by the peening treatment

Stress range $\Delta\sigma$ (MPa)	Improvement rate in air (%)	Improvement rate in 3.5 % NaCl (%)
160	8	19
115	27	32

sion resistance of the WM is attributed to its coarse grain and low hardness. Figure 10b shows the potentiostat curves for the welded samples with peening. As observed from the figure, the corrosion resistance of the three regions merged into a narrow range of potential. This suggests that the peening treatment significantly improved the corrosion resistance of the WM with coarse grains compared to the other regions.

3.4. Discussion on the effect of peening on fatigue and corrosion fatigue behavior

Figure 6 shows that the S-N curves for the welded specimens with and without peening under a 3.5 % NaCl solution environment are almost parallel, and the fatigue strength of the peened specimen is higher than that of the unpeened specimen. Based on the above corrosion resistance tests, it can be concluded that ultrasonic peening improves corrosion resistance. Therefore, since the corrosion effect does not significantly depend on stress level, it is speculated that the S-N curves become parallel. In contrast, the S--N curves for the welded specimens with and without peening in air are not parallel. At lower stress levels, the fatigue life of the peened specimen is longer than that of the unpeened specimen, while at higher stress levels, the fatigue lives for both peened and unpeened specimens converge, as shown in Fig. 6. This behavior is similar to the effect of residual stress on the S-N curve: at higher stress levels, the residual stress is relaxed, which offsets the balance of residual stress due to local plastic deformation. Therefore, the improvement of fatigue strength due to peening in air results from the residual stress induced by the peening treatment. The improvement in fatigue strength due to the peening treatment in a 3.5 % NaCl solution, as observed in Fig. 6, is attributed to the compressive residual stress induced by the peening and the hardening of the surface layer with the microstructure refinement.

The improvement rates of fatigue lives by the peening treatment were evaluated at high and low applied stress levels based on Figure 6 to determine which factor is dominant. The improvement rate of the fatigue life, ΔN_f, is defined as:

$$\Delta N_f = \{N_f(\text{with peening}) - N_f(\text{without peening})\} / N_f(\text{without peening}), \quad (1)$$

where N_f is defined as the number of cycles until failure at a given stress value.

The results are presented in Table 7. As discussed above, the improvement rate in air is mainly due to the compressive residual stress. Compared to that in air, the further improvement in a 3.5 % NaCl solution is mainly due to the surface hardening with refinement of the microstructure near the surface induced by the peening treatment.

4. Conclusions

In the present study, the effects of ultrasonic peening on the fatigue and corrosion fatigue of butt-welded 5086-H32 aluminum alloy were investigated in detail. Corrosion tests were also carried out to determine the effect of the peening treatment on corrosion behavior. Based on the results, the effects of residual stress and hardening induced by the peening treatment were successfully separated and analyzed in detail. The main conclusions of this study can be summarized as follows:

(1) Peening treatment improved fatigue strength in air and significantly enhanced corrosion fatigue strength in 3.5 % NaCl solution.

(2) Fatigue fractures were concentrated at the weld-toe, where stress is highest. Due to its thickness and sensitivity, the WM region showed severe corrosion at the fusion line.

(3) No exfoliation corrosion was detected, but significant intergranular corrosion was found in the WM and weld-toe regions.

(4) Without peening, WM had higher corrosion susceptibility than HAZ and BM, which decreased to similar levels post-treatment.

(5) Peening treatment increased fatigue strength at low stresses and enhanced corrosion fatigue strength at all stress levels through compressive residual stress and surface hardening.

Acknowledgements

This research was supported by FNSS Defence Systems. The authors would like to thank FNSS Defence Systems.

References

[1] S. J. Maddox, Review of fatigue assessment procedures for welded aluminium structures, Int. J. Fatigue 25 (2003) 1359–1378. https://doi.org/10.1016/S0142-1123(03)00063-X

[2] A. R. Shahani, I. Shakeri, C. D. Rans, Effect of residual stress redistribution and weld reinforcement geometry on fatigue crack growth of butt welded joints, Int. J. Fatigue 139 (2020) 105780. https://doi.org/10.1016/j.ijfatigue.2020.105780

[3] T. N. Nguyen, M. A. Wahab, The effect of weld geometry and residual stresses on the fatigue of welded joints under combined loading, J. Mater. Process. Technol. 77 (1998) 201–208. https://doi.org/10.1016/S0924-0136(97)00418-4

[4] R. C. McClung, A literature survey on the stability and significance of residual stresses during fatigue, Fatigue Fract. Eng. Mater. Struct. 30 (2007) 173–205. https://doi.org/10.1111/j.1460-2695.2007.01102.x

[5] H. Lin, J. R. Hwang, C. P. Fung, Fatigue properties of 6061-T6 aluminum alloy butt joints processed by vacuum brazing and tungsten inert gas welding, Adv. Mech. Eng. 8 (2016). https://doi.org/10.1177/1687814016643454

[6] C. M. Sonsino, D. Radaj, U. Brandt, H. P. Lehrke, Fatigue assessment of welded joints in AlMg 4.5 Mn aluminium alloy (AA 5083) by local approaches, Int. J. Fatigue 21 (1999) 985–899. https://doi.org/10.1016/S0142-1123(99)00049-3

[7] N. Sidhom, A. Laamouri, R. Fathallah, C. Braham, H. P. Lieurade, Fatigue strength improvement of 5083 H11 Al-alloy T-welded joints by shot peening: experimental characterization and predictive approach, Int. J. Fatigue 27 (2005) 729–745. https://doi.org/10.1016/j.ijfatigue.2005.02.001

[8] D. Živković, B. Anzulović, The fatigue of 5083 aluminium alloy welds with the shot-peening crater hot-cracks, Mater. Des. 26 (2005) 247–250. https://doi.org/10.1016/j.matdes.2004.02.003

[9] J. Schubnell, M. Farajian, Fatigue improvement of aluminium welds by means of deep rolling and diamond burnishing, Weld. World 65 (2021) 699–708. https://doi.org/10.1007/s40194-021-01212-1

[10] J. Kleiman, Y. Kudryavtsev, O. Luhovskyi, Effectiveness of ultrasonic peening in fatigue improvement of welded elements and structures, Mech. Adv. Technol. 3 (2017) 92–98. https://doi.org/10.20535/2521-1943.2017.81.117489

[11] K. Mutombo, M. Du Toit, Corrosion fatigue behaviour of aluminium alloy 6061-T651 welded using fully automatic gas metal arc welding and ER5183 filler alloy, Int. J. Fatigue 33 (2011) 1539–1547. https://doi.org/10.1016/j.ijfatigue.2011.06.012

[12] M. Mhaede, Influence of surface treatments on surface layer properties, fatigue and corrosion fatigue performance of AA7075 T73, Mater. Des. 41 (2012) 61–66. https://doi.org/10.1016/j.matdes.2012.04.056

[13] P. S. Prevéy, J. T. Cammett, The influence of surface enhancement by low plasticity burnishing on the corrosion fatigue performance of AA7075-T6, Int. J. Fatigue 26 (2004) 975–982. https://doi.org/10.1016/j.ijfatigue.2004.01.010

[14] M. Malaki, H. Ding, A review of ultrasonic peening treatment, Mater. Des. 87 (2015) 1072–1086. https://doi.org/10.1016/j.matdes.2015.08.102

[15] M. Daavari, S. A. Sadough Vanini, Corrosion fatigue enhancement of welded steel pipes by ultrasonic impact treatment, Mater. Lett. 139 (2015) 462–466. https://doi.org/10.1016/j.matlet.2014.10.141

[16] ASTM G66-99. Standard Test Method for Visual Assessment of Exfoliation Corrosion Susceptibility of 5XXX Series Aluminum Alloys (ASSET Test), ASTM International, (2013).

[17] American Society for Testing and Materials. Standard Test Method for Determining the Susceptibility to Intergranular Corrosion of 5XXX Series Aluminum Alloys by Mass Loss After Exposure to Nitric Acid (NAMLT Test), ASTM International, (2004).

[18] G. Xu, J. Qian, D. Xiao, Y. Deng, L. Lu, Z. Yin, Mechanical properties and microstructure of TIG and FSW joints of a new Al-Mg-Mn-Sc-Zr alloy, J. Mater. Eng. Perform. 25 (2016) 1249–56. https://doi.org/10.1007/s11665-016-1942-6

[19] X. Peng, X. Cao, G. Xu, Y. Deng, L. Tang, Z. Yin, Mechanical properties, corrosion behavior, and microstructures of a MIG-welded 7020 Al alloy, J. Mater. Eng. Perform. 25 (2016) 1028–1040. https://doi.org/10.1007/s11665-015-1863-9

[20] A. Abdullah, M. Malaki, A. Eskandari, Strength enhancement of the welded structures by ultrasonic peening, Mater. Des. 38 (2012) 7–18. https://doi.org/10.1016/j.matdes.2012.01.040

[21] A. V. Jebaraj, L. Ajaykumar, C. R. Deepak, K. V. Aditya, Enhancement of exfoliation corrosion resistance of aluminium alloy 5083 by shot peening, Surf. Rev. Lett. 25 (2018) 1950020. https://doi.org/10.1142/S0218625X19500203

[22] K. Sillapasa, S. Surapunt, Y. Miyashita, Y. Mutoh, N. Seo, Tensile and fatigue behavior of SZ, HAZ and BM in friction stir welded joint of rolled 6N01 aluminum alloy plate, Int. J. Fatigue 63 (2014) 162–70. https://doi.org/10.1016/j.ijfatigue.2014.01.021

[23] A. R. Shahani, I. Shakeri, Experimental evaluation of fatigue behaviour of thin Al5456 welded joints, Fatigue Fract. Eng. Mater. Struct. 43 (2020) 965–977. https://doi.org/10.1111/ffe.13173

[24] S. Amini, S. A. Kariman, R. Teimouri, The effects of ultrasonic peening on chemical corrosion behavior of aluminum 7075, Int. J. Adv. Manuf. Technol. 91 (2017) 1091–1102. https://doi.org/10.1007/s00170-016-9795-6

[25] W. Zhao, D. Liu, X. Zhang, Y. Zhou, R. Zhang, H. Zhang, C. Ye, Improving the fretting and corrosion fatigue performance of 300M ultra-high strength steel using the ultrasonic surface rolling process, Int. J. Fatigue 121 (2019) 30–38. https://doi.org/10.1016/j.ijfatigue.2018.11.017

[26] A. Goyal, R. K. Garg, Modeling and optimization of friction stir welding parameters in joining 5086 H32 aluminium alloy, Scientia Iranica 26 (2019) 2407–2417. https://doi.org/10.24200/SCI.2018.5525.1325

[27] V. Hans, P. S. Bajwa, Comparison of mechanical and corrosion behavior of aluminium alloy weldments, Int. J. Res. App. Sci. Eng. Technol. 6 (2018) 2900–2906. http://dx.doi.org/10.22214/ijraset.2018.3465

[28] Q. Wang, Y. Li, Z. Lu, Y. Zhang, Y. Zou, Effects of ultrasonic nanocrystal surface modification on mechanical and corrosion behavior of LZ91 Mg–Li alloy, Mater. Trans. 61 (2020) 1258–1264. https://doi.org/10.2320/matertrans.MT-M2019314

[29] P. S. Gowthaman, B. A. Saravanan, Investigation of processing action on Aluminium 5086 using Friction stir welding, Proceedings of International Conference on Emerging Trends in Science Technology Engineering and Management (2015), Trissur, India, pp. 1–8.

[30] Y. Huang, Y. Li, Z. Xiao, Y. Liu, Y. Huang, X. Ren, Effect of homogenization on the corrosion behavior of 5083-H321 aluminum alloy, J. Alloys Compd. 673 (2016) 73–79. https://doi.org/10.1016/j.jallcom.2016.02.228

[31] J. S. Kim, H. W. Lee, A study on effect of intergranular corrosion by heat input on Inconel 625 overlay weld metal, Int. J. Electrochem. Sci. 10 (2015) 6454–6564. https://doi.org/10.1016/S1452-3981(23)06732-9